Available online at www.sciencedirect.com
SCIENCE DIRECT®
PERGAMON
International Journal of Heat and Mass Transfer 46 (2003) 1425–1442
International Journal of HEAT and MASS TRANSFER
www.elsevier.com/locate/ijhmt

Periodicity and bifurcations in capillary tube boiling with a concentric heating wire

Narasimha Acharya [a,1], Mihir Sen [a], Eduardo Ramos [b,*]

[a] Department of Aerospace and Mechanical Engineering, University of Notre Dame, Notre Dame, IN 46556, USA
[b] Centro de Investigación en Energía, Ap. P. 34, Temixco, Morelos 62580, Mexico

Received 20 August 2001; received in revised form 30 August 2002

Abstract

Nucleate boiling from a vertical glass capillary in a pool of water is investigated here. Electrical heating is provided with a wire passing concentrically through the center of the capillary, and a fast-response thermocouple at the lip of the capillary records the instants of bubble departure. Different lengths and diameters of capillaries are used in the experiments. The average frequency of bubbling is seen to increase with applied heat flux, the relation being linear in the initial stages. With the heat flux used as a bifurcation parameter, one-dimensional return maps of the time interval between successive bubble emission events are used to study the transitions from the periodic state. The first bifurcation from the periodic to a two-period state is observed to be due to lateral instability of the liquid film adhering to the capillary wall. Further bifurcations to period two and then to period three bubbling are also observed. Simplified analysis of the different phases of the boiling process yields solutions which show close agreement with the experimental data.

1. Introduction

Boiling as a process has long been under study due to its many applications in industry. Extensive reviews of progress in boiling research have been provided by Collier [1], Cole [2], Hsu and Graham [3], Van Stralen and Cole [4] and Bergles et al. [5], among others. However, as pointed out by Lienhard [6] and Westwater [7], some of the basic mechanics of boiling are still unclear. Boiling is characterized by the creation of new liquid–vapor interfaces in the form of vapor bubbles. In nucleate boiling, these bubbles generally originate and grow from surface imperfections such as cracks or cavities containing entrapped gas or vapor. The present study seeks to analyse one aspect of this enormously complex problem: the qualitative and quantitative nature of bubbling in a confined volume. Even though the diameter of the capillary is larger than that of boiling cavity sizes, it is expected that some of our observations may contribute to understand the dynamics of bubbling in cavities. Also, it is unlikely to find that natural occurring crevases have cylindrical geometries, but nevertheless, this shape was chosen for simplicity. This is carried out within the framework of a simple experiment under carefully controlled conditions; the site should be of definite but variable geometry, and the heat input measurable. For these reasons, as well as for experimental simplicity, a cylindrical capillary structure with electrical heating was chosen for the present study. Observations in similar experimental arrangements have been reported in Acharya [8], Acharya et al. [9], Ramos et al. [10] and García et al. [11].

The basic mechanism involved in boiling within narrow vertical cavities has been studied by several workers. Wei and Preckshot [12] and Kosky [13] photographed bubble formation and growth to gain some insight into the dynamic behavior and stability of nucleating sites. Liquid penetration following bubble departure and the movement of the liquid–vapor interface within the capillary were studied. Increasing the system

* Corresponding author.
[1] Present address: Mattson Technology, San Jose, CA.

0017-9310/03/$ - see front matter
PII: S0017-9310(02)00400-3

Nomenclature

a	$= 3\nu/\Delta^2$
C_p	specific heat
g	acceleration due to gravity
L	distance of vapor penetration into capillary
L_m	total length of capillary
L_0	lowermost position of vapor slug in capillary
p	pressure
P_{av}	average driving pressure
q	heat influx per unit length from heater wire
q_b	heat flux at boiling
R	inner radius of capillary
t	time
δt	film characteristic time
T	temperature
T_0	initial bath temperature
T_{ext}	bath temperature
T_{sat}	saturation temperature
ΔT_b	temperature superheat over bath temperature
u	fluid velocity
u_L	velocity of lower vapor–liquid interface
U	proportionality constant for heat loss into bath
x	coordinate downward from capillary opening

Greek symbols

Δ	liquid film thickness adjacent to capillary
Δ_L	liquid film thickness at lower interface
μ	dynamic viscosity
ν	kinematic viscosity

pressure increased the liquid penetration as well as the bubble growth periods. A record was also obtained of bubble shapes which ranged from flattened at low pressures to spherical at high pressures. In the post-departure phase in the cavity, a vapor pocket was found to exist within the capillary following bubble departure, engendering further bubble formation. The importance of surface tension and hydrodynamic effects in necking down of the vapor column and the resulting bubble break-away were also pointed out.

Experiments on a flat slot have been performed by Aksyonova et al. [14] who studied the effect of slot width and heat input on bubble parameters. Departure diameters of bubbles were found to increase with decreasing slot thickness, and were found to increase linearly with applied flux. Growth rates were also found to increase with decrease in slot thickness and increase in heat flux. While investigating nucleate boiling from a flat slot at atmospheric pressure, Fujita et al. [15] observed a decrease in heat transfer with increasing lengths at high heat fluxes due to excessive vapor formation impeding liquid inflow into the slot. They also observed that as the slot spacing was decreased, the heat transfer first increased and then decreased suggesting that an optimal spacing exists for maximum heat transfer.

Schultz and Cole [16] conducted experiments on a 38 μm hole drilled into a zirconium ribbon. The initial growth rates of bubbles followed the criterion proposed by Mikiç et al. [17] for growth in a uniformly superheated thermal layer. From observations on nucleation instabilities, they concluded that the thermal boundary layer had little effect on growth itself except for incipience and initiation of growth. Some useful quantitative information regarding bubble growth [18–20] has also been gained through visualization.

The role of various parameters in influencing bubble frequencies has been investigated by several researchers. Shoukri and Judd [21] noticed that the effects of an increase in flux, decrease in cavity size and a decrease in liquid subcooling were to raise the bubble frequency. With higher fluxes, there is a larger heat available for evaporation; the rise in frequency due to the other factors was regarded as occurring due to a decrease in waiting time. However, it was pointed out that the influence of liquid subcooling is not very significant at low subcoolings since the liquid flowing into a site following bubble departure comes from the already superheated thermal layer; hence the effect is felt only indirectly in the time required to replenish this layer.

Photographic evidence of dichloromethane boiling off a heated glass surface enabled Judd and Hwang [22] to deduce the frequency along with departure diameter and active site density. These were then used in predicting the microlayer evaporation component of heat flux as part of a comprehensive model for nucleate pool boiling. Correlation of the experimental data obtained by Paul and Abdel-Khalik [23] for water undergoing nucleate boiling off a platinum wire indicated that the average bubble frequency had a power law relation with the applied flux.

An important finding of many of the experiments mentioned above is that under most conditions, frequency data exhibit considerable randomness in time. Many workers have remarked on the observed wide variation in bubble departure diameter and frequency under constant conditions. In one particular case, the periods of 86 bubbles observed at a particular site varied from 0.01 to 0.045 s [18]. In the same study, growth rates of vapor bubbles were also observed to exhibit significant variations. Cumo et al. [24] measured departure

diameters at various levels of liquid subcooling and found decreasing scatter of data with increasing subcooling. While supporting the trend of scatter in bubble sizes in saturated boiling off a platinum wire, Paul and Abdel-Khalik [23] also found a normal distribution of active nucleation sites on the heater surface at various heat fluxes. Additionally, Sultan and Judd [25] report that active sites have a Poisson distribution. These observations tend to encourage the view that nucleate boiling is random in nature. Lending support to this viewpoint are the experiments of Aksyonova et al. [14] on bubble generation from a flat slot, in which the frequency displayed a broad-band distribution.

There is evidence, on the other hand, that extremely regular periodicity is also possible. As an example, one can see some of the periodic sequences in the motion picture film on active boiling sites for pentane on zinc by Westwater and Strenge [26]. Acharya et al. [9] reported on a bifurcation from one periodic state to another in bubble emission from a nucleating glass capillary for low heat fluxes. Experimental observations in capillaries have been performed by Ramos et al. [10] using a device with a geometry similar to that in the present investigation, but with a heating wire loop located at the bottom of the capillary. A bifurcation from single to double frequency was identified. The main physical mechanism responsible for this behavior was the liquid accumulation at the bottom of the capillary that resulted in the expulsion of a liquid packet of water forcing the departure of a bubble even when the buoyancy was not enough to overcome the surface tension attachment force. Detailed observations of García et al. [11] in the same system revealed yet another physical mechanism that is also responsible for the disruption of the single frequency oscillatory behavior, namely waves that develop in the falling liquid films near the walls. In some events, waves with large enough amplitude obtrude the passage of vapor and form a liquid package that acts like a piston pushing the bubble in the process of formation. This mechanism has also been observed in the present paper. Recently, two symbolic dynamics models for predicting the statistical properties of the observations of Ramos et al. [10] have been published by Cordonet et al. [27]. Although a definite agreement between these models and experiments has not been reached, mostly due to incomplete experimental information, substantial progress towards a dynamical model has been achieved.

The companion problem of bubble detachment by controlled expulsion of gas from the bottom of a pool of water under isothermal conditions has been studied theoretically by Clausse et al. [28] and experimentally by Garea et al. [29]. Clausse et al. [28] propose a model based on an energy minimization principle to explain the detachment process. The experimental data of Garea et al. [29] indicate that the bubble detachment process changes from a periodic to chaotic state as the flow rate is increased. Another series of experiments on bubbling has been reported by Tritton and Egdell [30] who observed period doubling as a route to chaos.

With a similar philosophy, it is hypothesized that the heat flux may change the boiling process from a periodic to a stochastic regime. Dynamical systems theory has shown that there is no contradiction between deterministic models and aperiodicity. But before a model can be set up for predictions, it should be experimentally determined that boiling can indeed be made to go from periodic to aperiodic simply by changing a suitable parameter. One important parameter in the process is the heat flux which, if electrically generated, can be carefully controlled and continuously varied. However, one must ensure that all the heat generated actually enters the fluid. These aspects were sought to be resolved by the present experiments.

2. Experimental set-up

The experiments were conducted in a glass capillary tube, sealed at the bottom, immersed in a beaker of water maintained at a temperature T_{ext} of 98 °C by external heating with a thermostatically controlled hot plate. A steady bath temperature was obtained by adjusting the heat supplied to the beaker to balance the heat lost from its surface. The beaker is 15 cm in diameter and 20 cm in height. Fig. 1, not drawn to scale, displays a schematic of the experimental set-up with some of the relevant details. All surfaces were cleaned with acetone and then with distilled water prior to use.

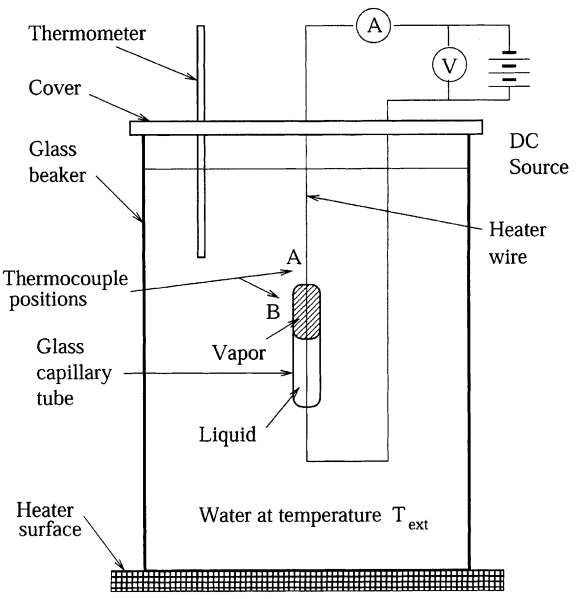

Fig. 1. Schematic of experimental set-up.

Distilled water was used for all runs and degassing was achieved by boiling the water for about 30 min before commencing the test runs. The capillary was held vertical by a clamp provided with level adjustment screws and the wire was maintained taut by tightening it against a screw on the cover plate. Two capillary diameters were used 1.23 and 1.40 mm. The lengths of the capillaries were 4–6 and 8 cm. Heat required for localized boiling at the capillary was supplied by passing a DC current through a 0.254 mm diameter, constantan wire located at the center of the capillary. Then, heat flux from the wire to the liquid is power per unit length. The wire was uniformly roughened with emery paper to discourage preferential nucleation at any particular spot on its surface. The electrical power input could be varied and measured by a voltmeter and ammeter arrangement. Detailed calculation indicates that thermal radiation loss is less than 3% of the total power supplied, and decreases as the power density increases. Axial conduction is less than 0.4% of the power input.

Temperature fluctuations at the lip of the capillary, induced by the passage of a vapor–liquid interface during bubbling, were sensed by a differential 75 μm diameter copper–constantan thermocouple. The two junctions of the thermocouple were placed at A and B so that the voltage produced at the thermocouple terminals was directly proportional to the temperature difference between those locations. This signal was amplified 104 times and stored in a Zenith PC for further processing. The measured time constant of the thermocouple was 25.5 ms, which was sufficient for the bubbling frequencies observed in the experiments reported here. The differential arrangement removed most of the effect of temperature fluctuations due to the motion of water outside the capillary arising due to natural convection and the mixing provoked by boiling. A video camera with a macro lens was also used for some runs for a close-up visual record of the boiling process.

The capillary bore was chosen so as to ensure that the motion of the vapor slug within the capillary was largely one-dimensional along its length. Since there is no curvature of the beaker or the capillary in the vertical direction, measurements made along this direction were practically free of image distortion. The bubble diameter measured in the horizontal direction was scaled in linear proportion with the lateral distortion of the capillary, which could be explicitly determined. The error introduced by such a calculation were small as the bubble diameters actually measured were close to the outer diameter of the capillary.

Fig. 2 shows part of a typical temperature trace from the thermocouple at low heating. Passage of the vapor bubbles corresponds to spikes in the trace, enabling an accurate determination of the interval between successive bubbles. In the example shown, the behavior is seen to be cyclic and roughly periodic. Quantitative information on the intervals between bubble emissions for any given run can be obtained by processing this data.

Observations on the oscilloscope showed negligible temperature variations in the low heat flux regime when the pool temperature was at or near saturation. As the liquid subcooling increased, so did the magnitude of the temperature spikes corresponding to bubble passage over the thermocouple. This suggests that the vapor superheat is small at low to moderate heat fluxes. Additionally use of the oscilloscope enables one to relate the temperature fluctuations to bubble emission. Observations showed the peaks to occur at instants when

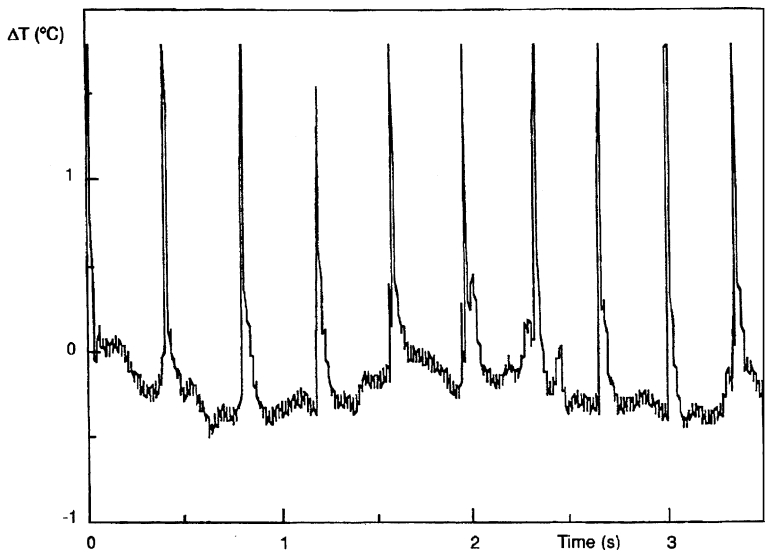

Fig. 2. Time trace of thermocouple output for a heat flux of 23.6 W/m.

the bubbles crossed the thermocouple junction. Thus the peaks in the temperature trace correspond to vapor superheat over the pool temperature.

3. Effect of heat and capillary length

As the heat flux was increased from zero, it was found that a threshold value had to be reached before boiling could commence. Following its initiation, however, boiling could be maintained at slightly lower fluxes, indicating some hysteresis in its onset.

The heat supplied through the wire into the capillary provides the driving force for the boiling process. Below the critical value required to initiate bubble emission, the heat supplied is dissipated by conduction through the surrounding liquid. Assuming steady radial conduction through the liquid and the capillary tube wall, the heat flux at the heater surface can be calculated as a function of the temperature excess of the heater surface over the pool temperature. Fig. 3 displays the linear relationship between this flux and the temperature excess. Also plotted on this diagram are the upper and lower bounds on the heat flux corresponding to the limits of variation of thermal conductivity for capillary glass material. Since the incipient flux was around 20 W/m for most cases, as shown in Fig. 3, the temperature at the heater wire surface at incipience could be estimated to be 7–9 °C above the pool temperature, i.e. between 105 and 107 °C.

Some previous models of boiling in cylindrical geometries [31–34] have assumed the formation of a vapor slug near the bottom of the cavity. In the present experiments, the vapor slug was formed and maintained near the top. Its growth was seen to occur by subsequent movement of both its lower and upper liquid–vapor interfaces, the lower one moving downwards into the cavity and displacing existing liquid and the upper interface forming the bubble. When the upper interface breaks off into a bubble, liquid rushes in to fill the cavity and the process begins again. Liquid motion out of the cavity and into it is through a film formed at the wall.

The average frequency was determined over the entire run by considering the mean bubble period of a large number of emission events. These are shown in Fig. 4 as functions of the heat flux for three different capillary lengths. It is observed that, in general, the frequency increases linearly with heat flux in the beginning before tending to level off. A second order fit is shown in each case. The linear part of the curve can be understood in principle if we assume that the energy per unit time removed by the vapor varies as its frequency, while the total heat generated is proportional to the product of the heat flux per unit length and the length of the capillary. As the movement of the lower interface brings it close to the bottom of the capillary for high heat fluxes, there is some non-linearity which affects this behavior, leading to the leveling off. It is also observed that the bubble frequencies increase with increasing capillary lengths, the effect being more pronounced at low heat fluxes.

The effect of capillary length on boiling discussed here is in contrast to the insensitivity observed in flat slots by Fujita et al. [15]. The reasons could be the

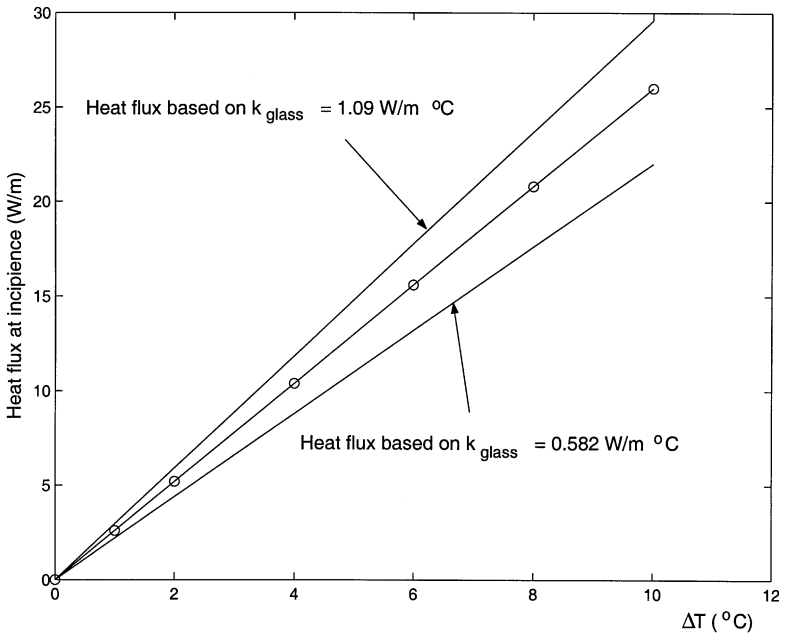

Fig. 3. Variation of incipient heat flux with heater surface temperature excess over pool temperature; capillary diameter = 1.23 mm.

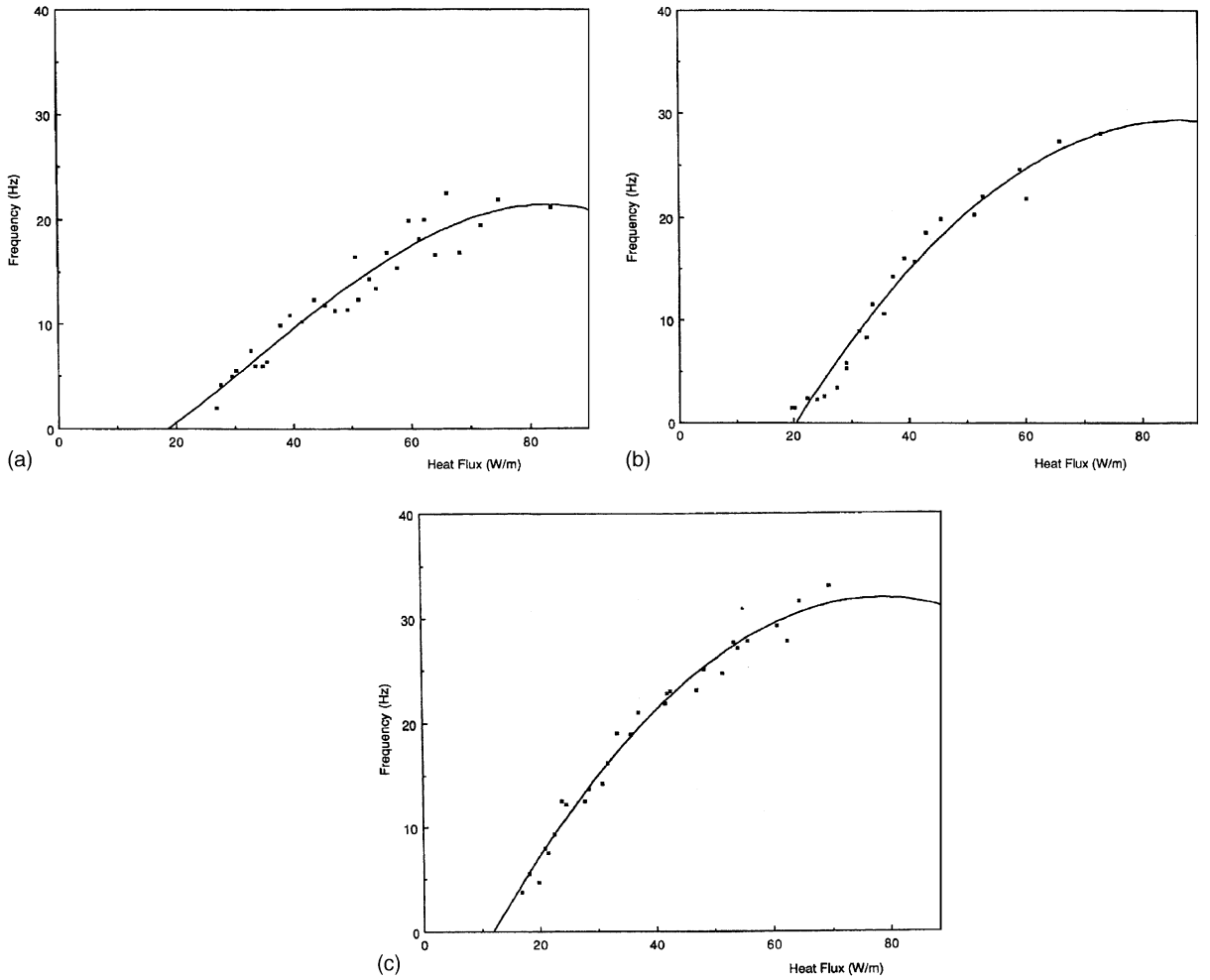

Fig. 4. Average bubble frequency variation with heat flux; capillary length (a) 3, (b) 5 and (c) 8 cm.

difference in geometry and heating arrangements in the two experiments.

4. Bifurcations from the periodic state

The emission phenomenon on commencement of boiling is seen in Fig. 2 to be periodic. This phenomenon was found to be reproducible in the very low heat flux range, although quantitatively the flux range for this to happen could change slightly, possibly due to change in surface characteristics of the heater wire and ambient conditions. With increasing heat fluxes, the periodic state bifurcates to a doubly periodic state with the upper interface moving at twice the frequency of the lower one. It must be noted that an extremely fine control is required over the heat flux in order to study the bifurcation. This is necessary since the heat flux range over which this occurs is narrow.

Fig. 5 shows the time series of the temperature difference registered by the thermocouple in differential mode for different heat fluxes. In Fig. 5(a) the phenomenon of bubble departure is periodic. On the other hand, in Figs. 5(b) and (c) it is seen that a cycle consists of two bubbles departures, a short interval followed by a longer one. It is observed that the demarcation between the periods becomes more pronounced as the flux is increased. In this regime, if one considers the alternate peaks in the time trace, it is noticed that they are relatively evenly spaced. A cycle may then be imagined as consisting of two events which occur in a definite relation to each other. The time period between adjacent bubbles computed for the whole range of observation yields two distinct values whereas the alternate periods within a cycle maintain a constant ratio.

It may be noticed that the use of the differential arrangement for the thermocouple means that a strong signal will result when a bubble traverses the probe while

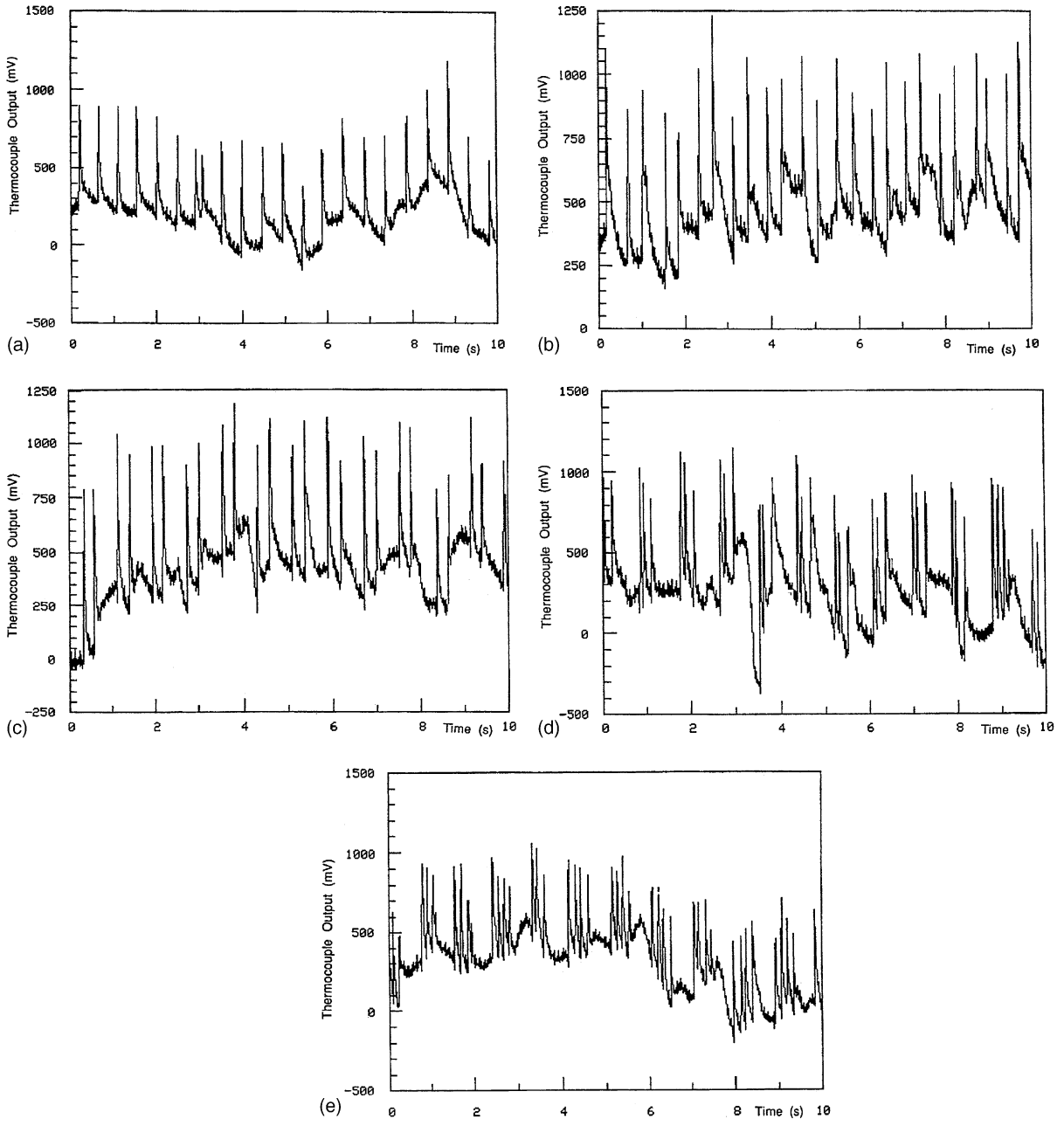

Fig. 5. Time trace of thermocouple output for various heat fluxes. (a) Heat flux = 14.74 W/m, (b) heat flux = 17.61 W/m, (c) heat flux = 21.79 W/m, (d) heat flux = 23.30 W/m and (e) heat flux = 24.22 W/m.

at other instants of time, the output, which is small, is masked by noise. The differential thermocouple therefore acts like an on–off switch capturing mainly the temperature pulses corresponding to bubble emission. This, combined with the fact that there is some scatter in the data as also the unequal amplitudes far corresponding peaks in the time trace, makes it difficult for a phase-plane study to demarcate the system behavior. However, periodicity of bubble departure can be examined by considering a series of maps (t_n, t_{n+1}) where t_n is the time period between successive bubble detachments. This is equivalent to chopping the continuous signal at discrete intervals and is somewhat similar to taking a Poincaré section of the data. In such a map the periodic state is represented by a single point with all points lying on top of one another. Fig. 6(a), for instance, shows the points gravitating

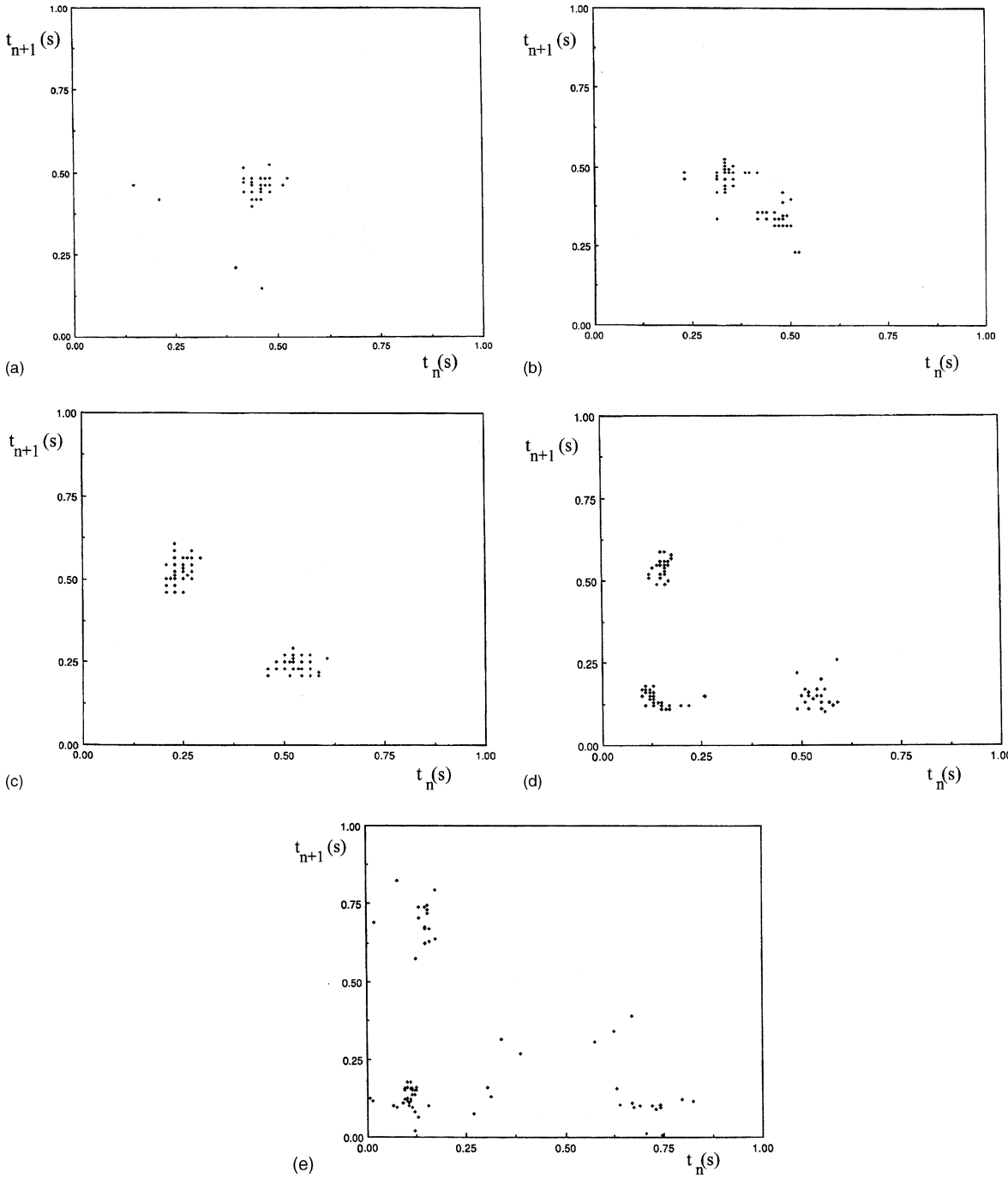

Fig. 6. Return maps of bubble periods: (a) Heat flux 14.74 W/m: 45 bubble cycles, (b) heat flux = 17.61 W/m: 86 bubble cycles, (c) heat flux = 21.79 W/m: 90 bubble cycles, (d) heat flux = 23.3 W/m: 90 bubble cycles and (e) heat flux = 24.22 W/m: 70 bubble cycles.

towards a single point corresponding to an average period of 0.45 s. Theoretically, a periodic signal is represented by a single point; however, in the present case, there is a slight spread observed about the ideal point. There are also a few points, less than 5%, outside the small region.

At a slightly higher heat flux, a decrease in periodicity was manifested by a gradual spreading of points in the map representing, perhaps, an instability of the periodic state. That the system is close to transition is borne out by Fig. 6(b) in which two distinct regions of dense points

are seen to have emerged. A given point in either one of these regions is mapped into the other and vice-versa. This shows a regime which has bifurcated to a doubly periodic state from the previously periodic one at a lower heat flux. The closeness of the two regions is indicative of the nearness of the system to the state at which this transition occurs. The bifurcation of the periodic state at this stage, which is not readily apparent from the time trace, is well clarified by the map.

As the heat flux is increased, the two groups of points seem to be moving apart in the map, as shown in Fig. 6(c), indicating the development to a stable doubly periodic state. In addition, an examination of the time traces shows that the ratio of the intervals between the two bubbles within a given cycle increases while the time interval between successive pairs of bubbles shows a small decrease. Within this regime, therefore, the frequency behavior shows little qualitative change, but due to the greater rate of bubble emission the average frequency is higher than that in the singly periodic case.

The onset of the doubly periodic regime occurs when, at a certain heat flux, the vapor slug in the capillary is pinched off near the top due to the lateral collapse of the liquid film at the wall. Under these conditions then there are two important processes that dictate bubble departure: one is the break-up of the bubble protruding from the top of the capillary which is influenced by surface tension and dynamic effects, the other is the localized necking of the vapor in the capillary due to the instability of the wall liquid film leading to the emission of a second bubble. Initially these two events are almost evenly spaced in time, but with an increase in heat flux the overall process is speeded up.

A further increase in heat flux at this stage leads to another transition. Compared to the doubly periodic case where the collapse of the liquid film gave rise to one extra bubble in a cycle, it is now seen that the collapse results in two or three additional bubbles. In this particular case, a large bubble is followed by a burst of two to three bubbles in quick succession followed by a delay when emission ceases. Following this, a group of three to four bubbles are emitted again and the process repeats. An illustration of the system behavior in this regime is depicted in the time traces, Figs. 5(d) and (e), and bubble period maps, Fig. 6(d), which now display three regimes of distinct points. Each of the graphs plotted here contain between 45 and 90 points which correspond to an identical number of bubble cycles. However, as many of these points lie one on top of another, they are not apparent in the graphs. Thus the concentration of experimental data points is actually much better than it looks.

In the maps portrayed above, there is a scatter leading to distinct regions of indistinct points. In other words, though it can be maintained with certainty that a given point in the map either returns to the same region as in the singly periodic case, alternates between the two regions as in the doubly periodic case, or rotates between three regions as in the triply periodic case, its exact location within the region is unknown, This scatter is much greater than the sampling resolution; it therefore indicates that the process is influenced by some random component.

The bifurcation diagram, Fig. 7, shows the evolution of the system as the heat flux is increased where the statistically averaged period is plotted as a function of the heat flux. In the singly periodic case, all periods between the bubbles are averaged; in the doubly periodic case, an averaging of alternate periods is resorted to, yielding two periods; in the triply periodic case, every third value is averaged, etc. The diagram obtained by plotting these periods against the bifurcation parameter, which in this case is the heat flux, is shown in Fig. 7. Within experimental error, the curve is seen to possess a pitchfork bifurcation, followed by a sequence of other bifurcations; the bars representing one standard deviation of the distribution of the bubble periods at that particular heat flux.

Data on the time period between successive bubbles were used for constructing bubble period histograms. Fig. 8 shows the series of histograms for the same capillary tube, but with different heat fluxes corresponding to the values of Figs. 6. In Fig. 8(a) the heat flux is low, the histogram is narrow indicating that the phenomenon of bubble formation and departure is periodic. The occurrence of a second peak in the histograms, Figs. 8(b) and (c), corresponds to the doubly periodic state; the three peaks in Fig. 8(d) to the period three state. The histograms are, in general, not symmetric, and there is a spread of bubble periods about the different mean values. The period four case, Fig. 8(e), appears to have only three distinct periods since two of them overlap in a common region at the lower end. The spread of these periods corresponds to scatter of points in the map.

These results show that the emission phenomenon undergoes a series of bifurcations as the heat flux is increased. They also show the existence of a random component giving rise to noisy periodicity at low heat fluxes. This random component arises due to practical limitations: non-constancy of the temperature during the test, natural convection effects, ambient temperature fluctuations, lack of purity of water used, and the dynamic effects of liquid motion generated as a result of boiling. Since liquid motion becomes more vigorous at higher heat fluxes, the effect of this on the observed periodicity also increases with heat flux.

5. Physical model

The physics of the formation and breakup of the vapor pocket can now be conjectured. The instantaneous

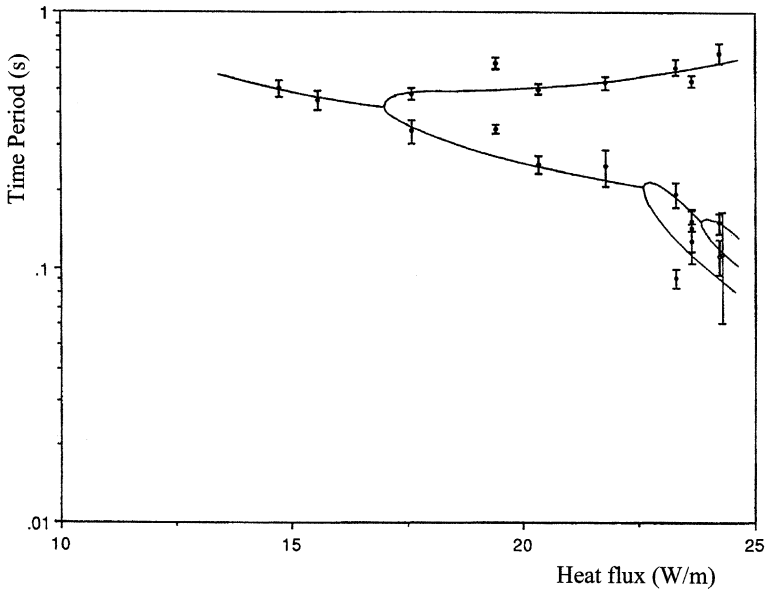

Fig. 7. Bifurcation diagram.

vaporization of a small volume of liquid adjacent to the heating wire results in a high pressure in the vapor, typically of the order of a few hundred atmospheres. This high pressure is primarily responsible for the expansion of the vapor into a growing slug. The vaporization process is thus accompanied by an expansion of the vapor pocket. As it expands, its upper surface swells breaking up eventually and emits a bubble. The lower interface, constrained to move along the tube length, descends much more rapidly into the capillary, pushing the liquid up along a film which is formed at the wall. After bubble break-off, there is liquid inflow into the cavity due to gravity and the lower interface moves up. Sometimes it is able to move all the way up to the top, and other times it reaches part of the way before the vapor begins to expand again and force it into a downward motion, when the cycle begins again.

At low heat fluxes, the upper and lower interfaces move in phase, and this activity gives rise to periodic bubble emission. As the heat flux is increased the vapor penetration into the cavity increases, probably indicating increased pressure in the vapor slug. A transition occurs at a certain value of the heat flux: the filling of the cavity cannot be completed due to instability of the wall film. Two bubbles are then formed for every period of the lower interface, with one of the bubbles being larger than the other. A typical thermocouple trace for bubble emission of this kind is shown in Fig. 5(c). The qualitative change in nature of the bubbling can be observed by comparing it with Fig. 2, which is at a lower heat flux; the single period of Fig. 2 has given way to two distinct periods in Fig. 5(c). It may be pointed out here that the previously mentioned movie by Westwater and Strenge [7] also shows a similar behavior for boiling on a flat surface. There is a sequence of a large bubble followed by a small one, the entire process repeating itself for a long time.

At still higher values of heat flux, there occur further transitions and eventually the bubble departure instants indicate a loss of periodicity. However, it appears that the lower interface motion continues to exhibit a tendency to remain periodic even for fluxes beyond which bubble emission is no longer periodic. Further increase of the heat flux results in the lower interface motion being affected and ultimately saturated by the finite capillary length.

Although there are some variations between cycles, the following stages can be identified within a cycle:

(1) A vapor bubble is generated; part of the vapor enters into the capillary, while the rest is expelled forming the first departing bubble.
(2) Liquid begins to fill the capillary; the vapor inside the capillary is displaced by the liquid.
(3) Bubble release; one or several bubbles may detach from the mouth of the capillary while the capillary fills up.

In order to illustrate this, Fig. 9 shows photographs of the bubble formation and departure at low heat fluxes at two different stages in the cyclic process. In Fig. 9(a), the vapor bubble is still attached to the capillary tube, while in Fig. 9(b), one bubble has left and another is

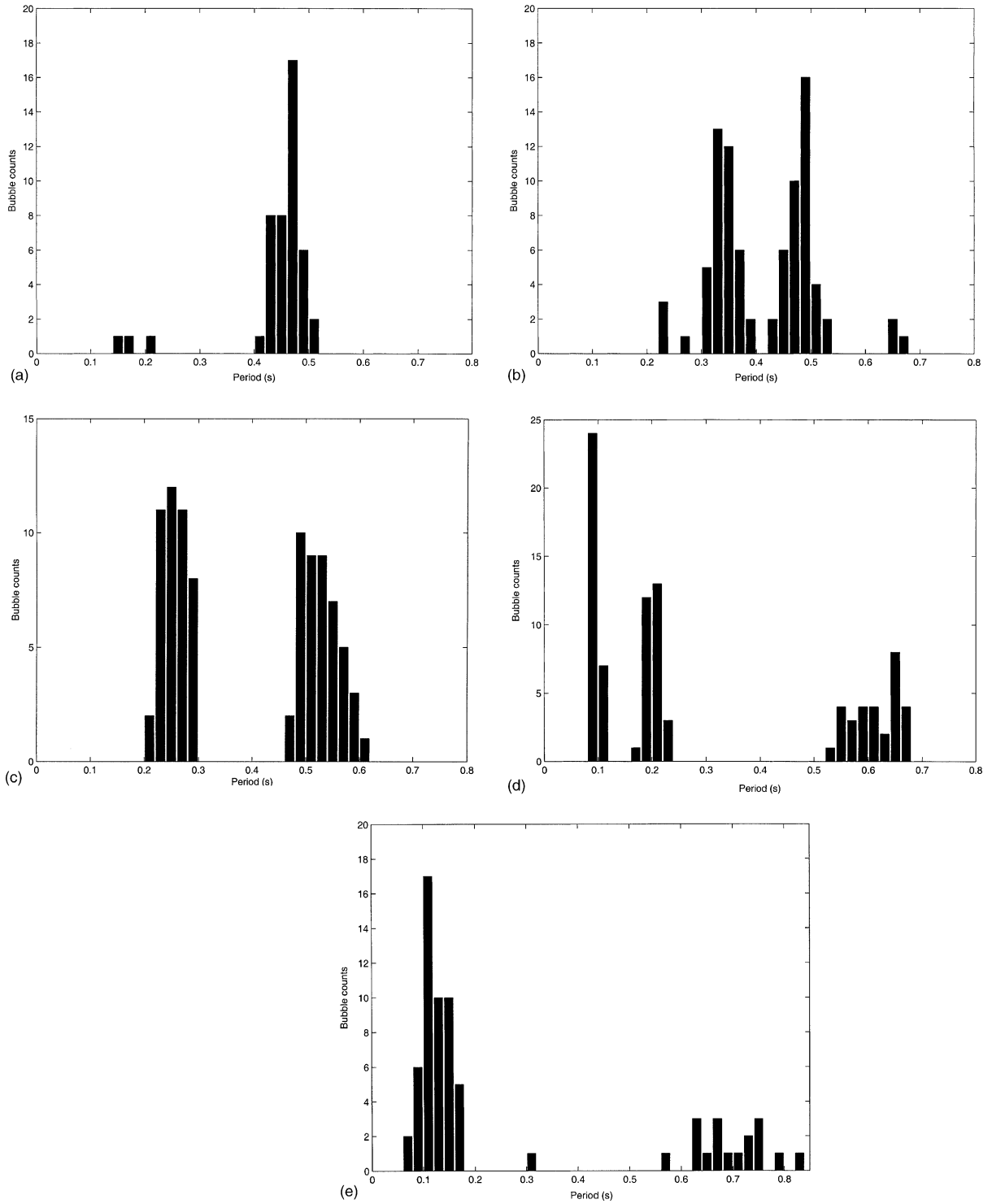

Fig. 8. Histogram of bubble periods; capillary length = 6 cm; capillary diameter = 1.4 mm. (a) heat flux = 14.74 W/m, (b) heat flux = 17.61 W/m, (c) heat flux = 21.79 W/m, (d) heat flux = 23.30 W/m and (e) heat flux = 24.22 W/m.

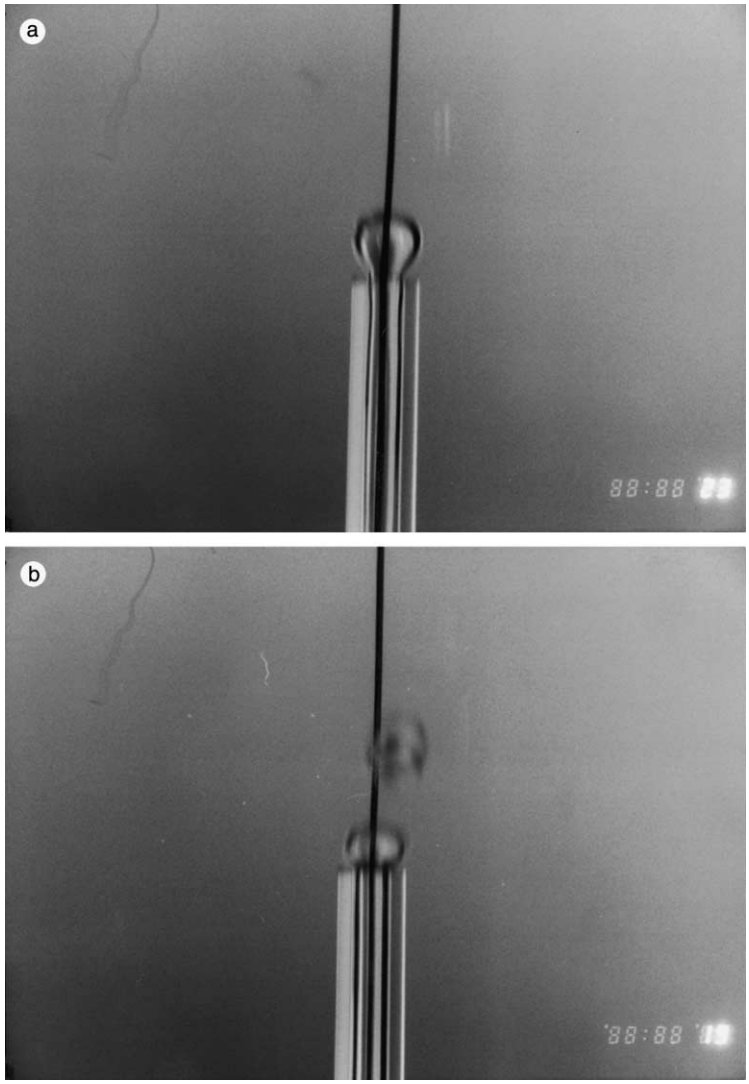

Fig. 9. Bubble formation and departure at low heat fluxes: (a) Bubble close to the moment of departure and (b) bubble after departure and early stage of formation of subsequent bubble.

being formed. The tube and central heating wire can be seen, as also the film of liquid at the wall of the tube.

6. Time scales in bubble generation

We consider the process of bubble generation. From experimental observations, we see that the bubble is generated on the wire surface at some position below the mouth of the capillary. We can divide this process into various stages. In the beginning, the bubble radius grows from approximately the radius of the heating wire to the radius of the capillary with a spherically symmetric and extremely rapid expansion. This is due to the high pressures generated within the vapor bubble. Using the balance between pressure and inertia forces [35], it is possible to determine that the characteristic time of this stage is $\sim 10^{-2}$ s. The subsequent expansion of the bubble, constrained by the capillary walls, is both upwards as well as downwards. The lower interface within the capillary displaces some liquid through an annular film; the upper interface forms the first departing bubble of that particular cycle.

Motion of the lower interface within the capillary exists so long as the pressure in the vapor phase exceeds that of the liquid. The maximum penetration depth is reached when the two pressures equilibrate. Assuming that the lower part of the bubble is hemispherical and that the liquid pressure is hydrostatic, the pressure balance is given by

$$\frac{2\sigma}{R} = \rho g L_0 \tag{1}$$

where σ is the surface tension coefficient, ρ the density of the liquid, R the radius of the capillary, g the acceleration due to gravity and L_0 is the maximum penetration depth. For a capillary radius of 0.7 mm, we find L_0 to be 18 mm which is approximately the range of values obtained experimentally. See Fig. 10. The expression is a static balance and does not take into account dynamic effects; as such the estimated L_0 is independent of the fluid velocity which is a result of the heat flux applied.

The total duration of this process can be calculated according to the following simple model: the downward moving bubble forces the liquid out of the capillary through a thin ascending film adjacent to the capillary wall. The motion is driven by the average pressure inside the bubble and resisted by the inertia of the liquid. This balance can be expressed as

$$\rho \pi R^2 L_0 \frac{L_0}{2\delta t^2} = P_{\mathrm{av}} \pi R^2 \tag{2}$$

where P_{av} is the average driving pressure, and the average acceleration is taken to be $L_0/2\delta t^2$. Taking $L_0 \sim 0.0138$ m for a heat input of 14.74 W/m from experimental observations and assuming $P_{\mathrm{av}} \sim 25$ MPa, the characteristic time is $\delta t \sim 6 \times 10^{-5}$ s. This is much smaller than the spherical expansion characteristic time, the reason being that in this case the expansion is one dimensional.

These order-of-magnitude estimates indicate that the bubble generation process lasts approximately 10 ms. Since the time resolution of the video camera is 30 ms and that of the thermocouple is 25 ms, details of the generation process cannot be experimentally recorded.

7. Analytical modeling

In describing the phenomenon with a simple model, two features that reflect the dynamics and heat transfer can be identified: motion of the upper and lower vapor–liquid interfaces respectively. The former is characterized by bubble release and the lower by motion inside the capillary. The heat carried away by the bubbles is the most important in terms of application. Even though the position of the lower interface is expected to critically influence the bubble dynamics, the converse is not true. In the following analysis, attention is focused on the position of the lower interface as a function of time.

Once the bubble has reached its maximum expansion inside the capillary, liquid flows in along the walls and vapor is pushed out through the mouth of the capillary. The liquid coming in is heated; if condensation is present, bubbles may or may not detach from the capillary, depending on vapor withdrawal at the bubble walls.

A schematic of the vapor bubble in the liquid inflow phase is shown in Fig. 11(a). Some geometrical simplifications, shown in Fig. 11(b), will be made to permit easy analysis: the vapor is separated from the lower liquid pool by a horizontal lower interface that is assumed flat, and from a cylindrical falling film by a vertical cylindrical surface. The origin of coordinates for

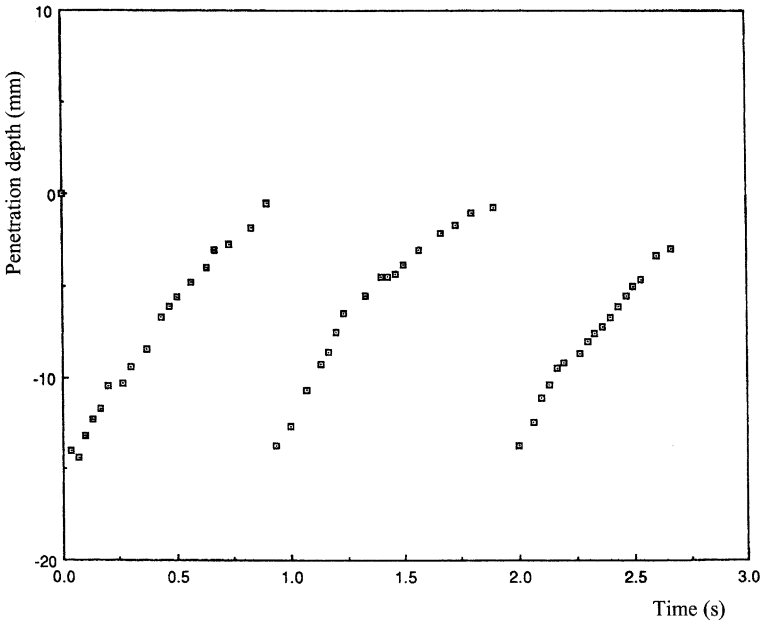

Fig. 10. Lower interface motion as a function of time; heat flux = 14.74 W/m.

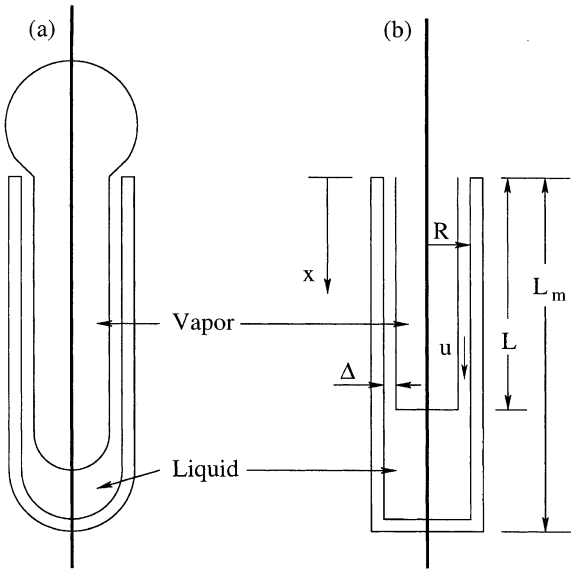

Fig. 11. Schematic of capillary tube and vapor bubble.

the x direction is at the tip of the capillary and is defined positive downwards. The thickness of the film is Δ. Typical dimensions are $L_m = 50$ mm and $R = 0.7$ mm.

Momentum balance for the falling film gives

$$\rho\left(\frac{\partial u}{\partial t} + u\frac{\partial u}{\partial x}\right) = -\frac{\mathrm{d}p}{\mathrm{d}x} - \frac{3\mu}{\Delta^2}u + \rho g \tag{3}$$

where the viscous force has been determined assuming a quadratic velocity profile in the film with a stress-free condition at the vapor–liquid interface. The vertical pressure gradient is due to the weight of the vapor column in the capillary and therefore negligible. Taking $u \sim \sqrt{2gL_0}$ and Δ to be 0.1 the viscous term is $\approx 5 \times 10^4$ N/m^3, while the gravity force term is 9810 N/m^3. Thus both the terms need to be retained. Neglecting the pressure gradient, we get

$$\frac{\partial u}{\partial t} + u\frac{\partial u}{\partial x} = g - au \tag{4}$$

where $a = 3\nu/\Delta^2$. Initial and boundary conditions are

$$u(x,0) = 0, \quad 0 < x < L_0 \tag{5}$$

$$u(0,t) = 0, \quad 0 \leqslant t \tag{6}$$

The solution has different forms in different regions of (x,t) space. The general solution of (4) is

$$\frac{\mathrm{e}^{-at}}{g-au} = f_1\left(x + \frac{u}{a} + \frac{g\ln|g-au|}{a^2}\right) \tag{7}$$

On using condition (5) this gives

$$f_1 = \frac{1}{g} \quad \text{and} \quad u = \frac{g}{a}(1-\mathrm{e}^{-at}). \tag{8}$$

Equivalently, the solution can be expressed as

$$x + \frac{u}{a} + \frac{g\ln|1-au/g|}{a^2} = f_2\frac{\mathrm{e}^{-at}}{g-au} \tag{9}$$

which on applying (6) gives

$$f_2 = \frac{g\ln g}{a^2} \tag{10}$$

and

$$x + \frac{u}{a} + \frac{g\ln|1-au/g|}{a^2} = 0. \tag{11}$$

The delimiting characteristic separating these two regions is when the velocities are equal, i.e. when

$$x - \frac{gt}{a} + \frac{g}{a^2}(1-\mathrm{e}^{-at}) = 0 \tag{12}$$

Thus

$$u = \frac{g}{a}(1-\mathrm{e}^{-at}) \quad \text{for } x - \frac{gt}{a} + \frac{g}{a^2}(1-\mathrm{e}^{-at}) > 0 \tag{13}$$

and

$$x + \frac{u}{a} + \frac{g\ln|1-au/g|}{a^2} = 0 \quad \text{for } x - \frac{gt}{a} + \frac{g}{a^2}(1-\mathrm{e}^{-at}) < 0 \tag{14}$$

On examining the above equations, it is clear that Eq. (13) is valid for short times while (14) is the long time solution. We shall use this together with the constraints specified in Eqs. (13) and (14) to construct the solution.

We neglect any condensation on the vapor–liquid interface; therefore the rate of increase of the mass of liquid in the lower pool is equal to the mass flow rate coming down the falling film. Thus

$$\frac{\mathrm{d}}{\mathrm{d}t}[\rho\pi R^2(L_m - L)] = \rho 2\pi R\Delta_{\mathrm{L}}u_{\mathrm{L}} \tag{15}$$

where Δ_{L} and u_{L} are measured at $x = L$. Also we have assumed that $\Delta_{\mathrm{L}} \ll R$. Simplifying, we get

$$\frac{\mathrm{d}L}{\mathrm{d}t} = -\frac{2\Delta_{\mathrm{L}}}{R}u_{\mathrm{L}}. \tag{16}$$

Eqs. (13)–(15) are solved simultaneously to obtain the velocity, u_{L}, and the location of the lower interface, L, as a function of time.

Fig. 12 shows experimental data compared to that indicated by solution of Eqs. (13)–(15). L_0 was measured to be 13.8 mm and $\Delta/R = 0.091$ was determined from a least squares fit. For $\Delta = 0.091$ mm, one finds that the parameter $a = 108.68$ so that a large parameter approximation for a can be invoked to simplify the expressions for the velocity (14) as

$$u = \frac{g}{a}(1-\mathrm{e}^{-a^2x/g}) \tag{17}$$

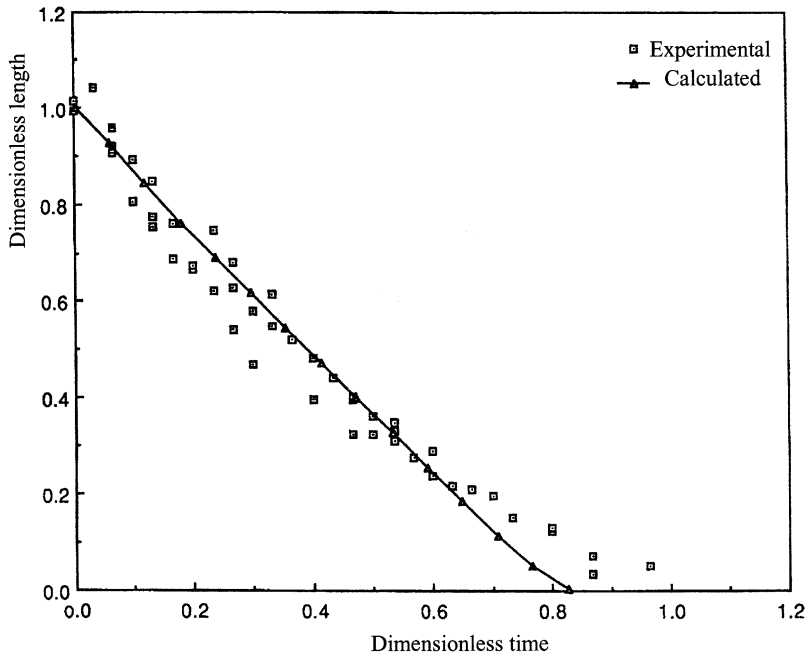

Fig. 12. Comparison of experimental and predicted variation of lower interface position as a function of time.

The lower interface position, L, can be represented as

$$L = L_0 + \frac{2g\Delta}{Ra^2}[1 - at - e^{-at}] \quad \text{for } L - \frac{gt}{a} + \frac{g}{a^2}(1 - e^{-at}) > 0 \tag{18}$$

and

$$L = \frac{g}{a^2}\ln\left[1 + \exp\left(\frac{a^2 L_0}{g} - 1\right)\exp\left(\frac{-2\Delta at}{R}\right)\right] \quad \text{for } L - \frac{gt}{a} + \frac{g}{a^2}(1 - e^{-at}) < 0 \tag{19}$$

In this analysis, the film thickness, Δ, has been assumed to be a constant both in time and in space. However, if the film thickness is allowed to vary with time, a better agreement may be obtained between the theoretical predictions and the experimental data over the complete cycle.

8. Energy balance

The temperature of the liquid inside the capillary determines the occurrence of the phase change and therefore the frequency of the bubble generation. In order to propose a simple model for the temperature inside the capillary, the following assumptions will be made. At the beginning of a cycle, the liquid pool in the capillary is assumed to be in equilibrium with the bath temperature. From then on the temperature in the liquid pool is determined by the heat input due to the heating wire, the mass of incoming liquid from the falling film, and the heat losses to the surroundings. It will be assumed that the liquid pool is a cylinder with a base area of πR^2 and height $L_m - L$ with a heat source located in the axis. If axial symmetry and large radial conduction are assumed, and natural convection neglected, the temperature field in the pool depends only on time and on the axial coordinate. The mass influx from the falling film is calculated from Eqs. (13) and (14) and it is assumed that there are heat losses to the surroundings that follow a linear relation governed by an overall heat transfer coefficient U. The temperature of the liquid falling into the capillary is calculated from a global energy balance

$$\rho\pi R^2 C_p(L_m - L)\frac{dT}{dt} = [q - 2\pi RU(T - T_0)](L_m - L) \tag{20}$$

with the initial condition

$$T(0) = T_0 \quad \text{at } t = 0 \tag{21}$$

Eq. (20) can be integrated in time starting from the initial condition (21) to obtain values of T at any subsequent time

$$T = T_0 + \frac{q}{2\pi RU}[1 - \exp(-2Ut/\rho C_p R]). \tag{22}$$

At incipient boiling we have

$$q_b = [(T_{sat} + \Delta T_b) - T_0]2\pi RU \tag{23}$$

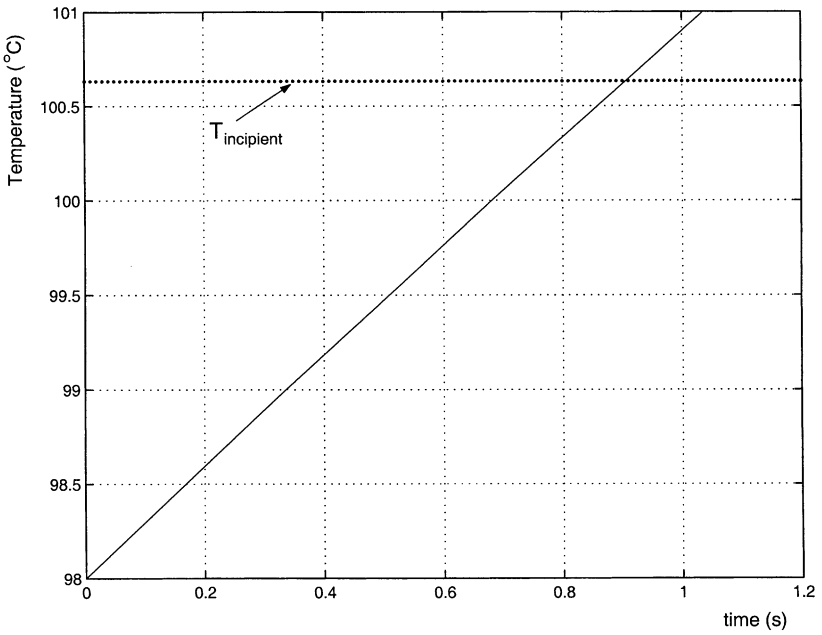

Fig. 13. Pool temperature as a function of time: $T_{\text{incipient}} = 100.63$ °C, heat flux = 14.74 W/m and capillary diameter = 1.23 mm.

where q_b and ΔT_b are the heat flux and overheat at boiling, respectively. The quantitative values for U and ΔT_b are obtained from the experimental data on incipient q vs. $T_{sat} - T_0$ reported Adams et al. [36]. The values for U and ΔT_b are 99.5 W/m^2 K and 0.633 °C respectively.

Fig. 13 shows the temperature field as a function of time. The criterion for the occurrence of phase change, i.e. generation of a new bubble, is when the temperature at any point inside the pool exceeds ΔT_b of superheat. Setting $T = T_{sat} + \Delta T_b$ and solving for time yields

$$t = -\frac{\rho C_p R}{2U} \ln\left(1 - \frac{T_{sat} + \Delta T_b - T_0}{q/2\pi RU}\right) \tag{24}$$

which gives $t = 0.9$ s for the particular parameters in this study. This agrees well with the experimental data which indicate that the cycle repeats at intervals of 0.85–0.9 s.

9. Conclusions

The capillary tube boiling experiment represents one of the simplest possible manifestations of nucleate boiling. Its advantages include the fact that convective interactions with the liquid in the pool are kept to a minimum. All the heat supplied by the electrical wire goes into the fluid so that the heat rate can thus be used experimentally as a bifurcation parameter. Most of the fluid motion is one-dimensional and thus easier to analyze in principle. With these simplifications, it becomes perhaps easier to understand qualitatively and quantitatively the mechanism of boiling, vapor formation and emission.

The results of the present experiments have indicated the variation of the average bubble departure frequency with heat flux. The idea of a low-dimensional behavior of the boiling phenomenon in the low heat flux regime is supported. Periodicity of bubble emission with a bifurcation to a doubly periodic state has been obtained. Subsequent bifurcations have also been observed. Frequency histograms indicate that the periodicity is interspersed with a small random component. The motion of the lower interface is seen to play a crucial role in the process.

There are some similarities and differences between the observations of capillary boiling with a concentric heating wire presented here and those from capillary boiling with extra heating at the bottom of the capillary reported by Ramos et al. [10] and García et al. [11]. When heating is made with a linear heat source, the upper and lower liquid–vapor interfaces of the vapor bubble inside the capillary play important dynamical roles; the relative frequency of the oscillatory motion of each interface seems to be responsible for the period doubling of the bubble departure. In contrast, when heat is supplied at the bottom, there is only liquid–vapor interface, and therefore the bubble departure mechanism is governed by the motion of the upper liquid–vapor interface. In this case, double periodicity in bubble departure is generated by liquid accumulation and expulsion. From the two investigations it can be concluded that the mechanisms leading to period doubling are

different in the two geometries. On the other hand, the observation that wave-like instabilities of large amplitude may trigger the departure of bubbles before buoyancy force overcomes surface tension is common to the two observations. This mechanism adds an stochastic component to the experimental data.

One part of the cyclic phenomenon, that relating to liquid fill-up in the capillary, has been modeled. Qualitative comparison with experimental results is good. However, the complete phenomenon in all its details is very complex and needs a more detailed study.

Acknowledgements

The authors gratefully acknowledge support from the NSF under grant number CBT-8515045 for this project. This research was also partly supported by NSF under INT90-01983 and by CONACYT (Mexico) under project G0044-E.

References

[1] J.G. Collier, Convective Boiling and Condensation, McGraw-Hill, New York, 1972.
[2] R. Cole, Boiling nucleation, in: Advances in Heat Transfer, vol. 10, Academic Press, New York, 1974, pp. 85–166.
[3] Y.Y. Hsu, H.W. Graham, Transport Processes in Boiling Systems, Hemisphere Publishing Corporation, Washington, DC, 1976.
[4] S.V. Van Stralen, R. Cole, in: Boiling Phenomena, vols. 1 and II, Hemisphere Publishing Corporation, Washington DC, 1979.
[5] A.E. Bergles, J.C. Collier, J.M. Delhaye, C.F. Hewitt, F. Mayinger, Two-phase Flow and Heat Transfer in the Power and Process Industries, Hemisphere Publishing Corporation, Washington, DC, 1981.
[6] J.H. Lienhard, Things we don't know about boiling heat transfer, Int. Comm. Heat Mass Transfer 15 (1988) 401–428.
[7] J.W. Westwater, Boiling heat transfer, Int. Comm. Heat Mass Transfer 15 (1988) 381–400.
[8] N. Acharya, Investigation of nucleate boiling from capillary tubes, M.S. Thesis, Department of Aerospace and Mechanical Engineering, University of Notre Dame, Notre Dame, IN 46556, 1989.
[9] N. Acharya, M. Sen, H.C. Chang, Experiments on the enhancement of heat transfer in coiled tubes by chaotic mixing, in: Fundamentals of Forced Convection Heat Transfer, HTD vol. 181, 1989, pp. 79–84.
[10] E. Ramos, P. Parmananda, G. Hernandez-Cruz, M. Sen, Dynamics of boiling from a short capillary tube, Exp. Heat Transfer 10 (1997) 273–290.
[11] J.M. García, G. Hernández-Cruz, E. Ramos, R. Rechtman, Visualization of capillary boiling, Exp. Fluids 30 (2001) 359–364.
[12] C.C. Wei, C.W. Preckshot, Photographic evidence of bubble departure from capillaries during boiling, Chem. Engng. Sci. 19 (1964) 838–883.
[13] P.C. Kosky, Nucleation site instability in nucleate boiling, Int. J. Heat Mass Transfer 11 (1965) 929–932.
[14] E.S. Aksyonova, M. D. Diev, B. M. Mironov, Internal characteristics of squeezed boiling, in: Proceedings of the 6th International Heat Transfer Conference, vol. 1, 1978, pp. 169–173.
[15] Y. Fujita, H. Ohta, S. Uchida, Heat transfer in nucleate boiling within a vertical narrow space, JSME Int. J. 31 (3, series 2) (1988) 513–519.
[16] R.R. Schultz, R. Cole, Bubble nucleation and growth instabilities in transient boiling, in: Proceedings of the 6th International Heat Transfer Conference, vol. 1, 1978, pp. 133–138.
[17] B.B. Mikiç, W.M. Rohsenow, P. Griffith, On bubble growth rates, Int. J. Heat Mass Transfer 13 (1970) 657–666.
[18] P.H. Strenge, A. Orell, J.W. Westwater, Microscopic study of bubble growth during nucleate boiling, AIChE J. 7 (4) (1961) 578–583.
[19] K. Stephan, M. Körner, Bubble frequencies during boiling of pure liquids and binary liquid mixtures, Wärme- und Stoffübertragung 3 (1970) 185–190.
[20] A. König, R. Gregorig, On the departure of steam bubbles under conditions of pool boiling, Wärme- und Stoffübertragung 6 (1973) 165–174.
[21] M.S.M. Shoukri, R.L. Judd, A theoretical model for bubble frequency in nucleate pool boiling including surface effects, in: Proceedings of the 6th International Heat Transfer Conference, vol. 1, 1978, pp. 145–150.
[22] R.C. Judd, K.S. Hwang, A comprehensive model for nucleate pool boiling heat transfer including microlayer evaporation, ASME J. Heat Transfer 98 (1976) 624–629.
[23] D.D. Paul, S.I. Abdel-Khalik, A statistical analysis of saturated nucleate boiling along a heated wire, Int. J. Heat Mass Transfer 26 (4) (1983) 509–519.
[24] M. Cumo, G. Farello, G.C. Pinchera, Some aspects of free convection boiling heat transfer, in: Proceedings of the 3rd International Heat Transfer Conference, vol. 3, 1966, pp. 225–238.
[25] M. Sultan, R.L. Judd, Spatial distribution of active sites and bubble flux density, ASME J. Heat Transfer 100 (1978) 56–62.
[26] J.W. Westwater, P.H. Strenge, Active Sites and Bubble Growth during Nucleate Boiling 16 mm Movie, Engineering Societies Library, New York, 1958.
[27] A. Cordonet, R. Lima, E. Ramos, Two models for the dynamics of boiling in a short capillary tube, Chaos 11 (2) (2001) 344–350.
[28] A. Clausse, The departure of a bubble viewed as a critical phenomenon, in press.
[29] V. Garea, F. Bonetto, A. Clausse, J. Converti, Periodic and chaotic states in bubbling dynamics, in: Proceedings of Congress on Fluids Experiments, Dubrovnik, 1991.
[30] D.J. Tritton, C. Egdell, Chaotic bubbling, Phys. Fluids A 5 (1993) 503.
[31] S.G. Bankoff, The prediction of surface temperatures at incipient boiling, Chem. Engng. Prog. Symp. Ser. 29 (55) (1959) 87–94.
[32] W.D. Ford, H.K. Fauske, S.G. Barkoff, The slug expulsion of Freon-113 by rapid depressurization of a vertical tube, Int. J. Heat Mass Transfer 14 (1971) 133–140.

[33] P.J. Marto, W.M. Rohsenow, Nucleate boiling instability of alkali metals, ASME J. Heat Transfer 88 (1966) 83–195.
[34] T.S. Playle, Simulation of sodium boiling using a water model: voiding and reentry processes, Chem. Engng. Sci. 28 (1973) 1199–1211.
[35] M.S. Plesset, S.A. Zwick, The growth of vapor bubbles in superheated liquids, J. Appl. Phys. 25 (4) (1954) 493–500.
[36] L.J. Adams, M. Sen, N. Acharya, Observations of boiling in a capillary U-tube, in: Proceedings of the ASME-JSME Thermal Engineering Joint Conference, vol. 2, 1991, pp. 289–293.